OPEN ACCESS

International
Journal
Of Modern Engineering Research (IJMER)

Single-Input Double Output High Efficient Boost Dc–Dc Converter

Thulasi V. S.[1], H. Satish kumar[2]

[1](Student, Department of Electrical and Electronics Engineering, FISAT, MG university, Kerala, India))
[2](Assistant Professor, Department of Electrical and Electronics Engineering, FISAT, MG university, Kerala, India)

ABSTRACT: *The aim of this project is to develop a high-efficiency single-input multiple-output (SIMO) dc–dc converter. The proposed converter can boost the voltage of a low-voltage input power source to a controllable high-voltage dc bus and middle-voltage output terminals. The high-voltage dc bus can take as the main power for a high-voltage dc load or the front terminal of a dc–ac inverter.Moreover, middle-voltage output terminals can supply powers for individual middle-voltage dc loads or for charging auxiliary power sources (e.g., battery modules). In this project, a coupled-inductor based dc–dc converter scheme utilizes only one power switch with the properties of voltage clamping and soft switching, and the corresponding device specifications are adequately designed. As a result, the objectives of high-efficiency power conversion, high step up ratio, and various output voltages with different levels can be obtained.*

Keywords: *Coupled inductor, high-efficiency power conversion, single-input multiple-output (SIMO) converter, soft switching, voltage clamping.*

I. Introduction

In order to protect the natural environment on the earth, the development of clean energy without pollution has the major representative role in the last decade. By dealing with the issue of global warning, clean energies, such as fuel cell (FC), photovoltaic, and wind energy, etc., have been rapidly promoted. Due to the electric characteristics of clean energy, the generated power is critically affected by the climate or has slow transient responses, and the output voltage is easily influenced by load variations.For example Photovoltaic (PV) sources are used today in many applications from satellite power systems to battery chargers and home appliances. The power produced by a solar panel depends on two factors;irradiation,and temperature. As irradiation and temperature levels change rapidly, the voltage produced fluctuates and becomes inconstant.

A converter is therefore required to produce a constant voltage that is matched to the requirements of the load and supplied efficiently. Therefore dc–dc converters with steep voltage ratio are usually required in many industrial applications. The conventional boost converters cannot provide such a high dc-voltage ratio due to the losses associated with the inductor, filter capacitor, main switch, and output diode.As a result, the conversion efficiency is degraded, and the electromagnetic interference (EMI) problem is severe under this situation.This study presents a newly designed SIMO converter(Boost converter) with a coupled inductor. Patra *et al.* presented "Single inductor multiple output switcher with Simultaneous Buck, Boost, and Inverted Outputs ".Which is capable of generating buck, boost, and inverted outputs simultaneously.However, over three switches for one output were required. This scheme is only suitable for the low output voltage and power application, and its power conversion is degenerated due to the operation of hard switching.

II. Literature Review

Nami et al. proposed "Multi-output DC–DC converters based on diode-clamped converters configuration topology and control strategy" a new dc–dc multi-output boost converter, which can share its total output between different series of output voltages for low- and high-power applications. Unfortunately, over two switches for one output were required, and its control scheme was complicated. Besides, the corresponding output power cannot supply for individual loads independently. Chen et al. "The Multiple-Output DC–DC Converter With Shared ZCS Lagging Leg" investigated a multiple-output dc–dc converter with shared zero-currentswitching (ZCS) lagging leg. Although this converter with the soft-switching property can reduce the switching losses, this combination scheme with three full-bridge converters is more complicated, so that the objective of high-efficiency power conversion is difficult to achieve, and its cost is inevitably increased.

This study presents a newly designed SIMO converter with a coupled inductor. The proposed converter uses one power switch to achieve the objectives of high-efficiency power conversion, high step-up ratio, and different output voltage levels. In the proposed SIMO converter, the techniques of soft switching and voltage

clamping are adopted to reduce the switching and conduction losses via the utilization of a low-voltage-rated power switch with a small *R*DS(on) . Because the slew rate of the current change in the coupled inductor can be restricted by the leakage inductor, the current transition time enables the power switch to turn ON with the ZCS property easily, and the effect of the leakage inductor can alleviate the losses caused by the reverse-recovery current. Additionally, the problems of the stray inductance energy and reverse-recovery currents within diodes in the conventional boost converter also can be solved, so that the high-efficiency power conversion can be achieved. The voltages of middle-voltage output terminals can be appropriately adjusted by the design of auxiliary inductors; the output voltage of the high-voltage dc bus can be stably controlled by a simple proportional-integral (PI) control.

III. Converter Design and Analyses

The system configuration of the proposed high-efficiency SIMO converter topology to generate two different voltage levels from a single-input power source is depicted in Fig. 2. This SIMO converter contains five parts including a low-voltage-side circuit (LVSC), a clamped circuit, a middle-voltage circuit, an auxiliary circuit, and a high-voltage-side circuit (HVSC). The major symbol representations are summarized as follows. $V_{FC}(I_{FC})$ and $V_{01}(I_{01})$ denote the voltages (currents) of the input power source and the output load at the LVSC and the auxiliary circuit, respectively; V_{02} and I_{02} are the output voltage and current in the HVSC. C_{FC}, C_{01} , and C_{02} are the filter capacitors at the LVSC, the auxiliary circuit, and the HVSC, respectively; C_1 and C_2 are the clamped and middle-voltage capacitors in the clamped and middle-voltage circuits, respectively. L_P and L_S represent individual inductors in the primary and secondary sides of the coupled inductor *Tr* , respectively, where the primary side is connected to the input power source; Laux is the auxiliary circuit inductor. The main switch is expressed as S_1 in the LVSC; the equivalent load in the auxiliary circuit is represented as R_{01},and the output load is represented as R_{02} in the HVSC. The corresponding equivalent circuit given in Fig. 2 is used to define the voltage polarities and current directions. The coupled inductor in Fig. 1 can be modeled as an ideal transformer including the magnetizing inductor Lmp and the leakage inductor Lkp in Fig. 2. The turns ratio N and coupling coefficient k of this ideal transformer are defined as

$$N = \frac{N_2}{N_1} \qquad (1)$$

$$K = \frac{L_{mp}}{L_{kp} + L_{mp}} = \frac{L_{mp}}{L_P} \qquad (2)$$

where N1 and N2 are the winding turns in the primary and secondary sides of the coupled inductor *Tr* . Because the voltage gain is less sensitive to the coupling coefficient and the clamped capacitor *C*1 is appropriately selected to completely absorb the leakage inductor energy , the coupling coefficient could be simply set at one (*k* = 1) to obtain Lmp = LP via (2). In this study, the following assumptions are made to simplify the converter analyses: 1) The main switch including its body diode is assumed to be an ideal switching element; and 2) The conduction voltage drops of the switch and diodes are neglected.

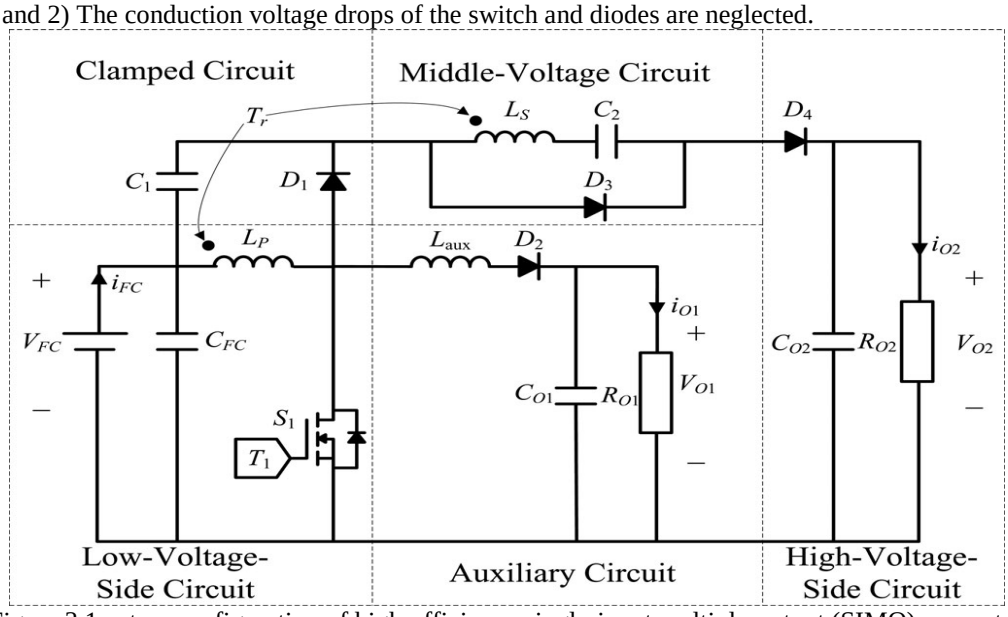

Figure 3.1: stem configuration of high-efficiency single-input multiple-output (SIMO) converter

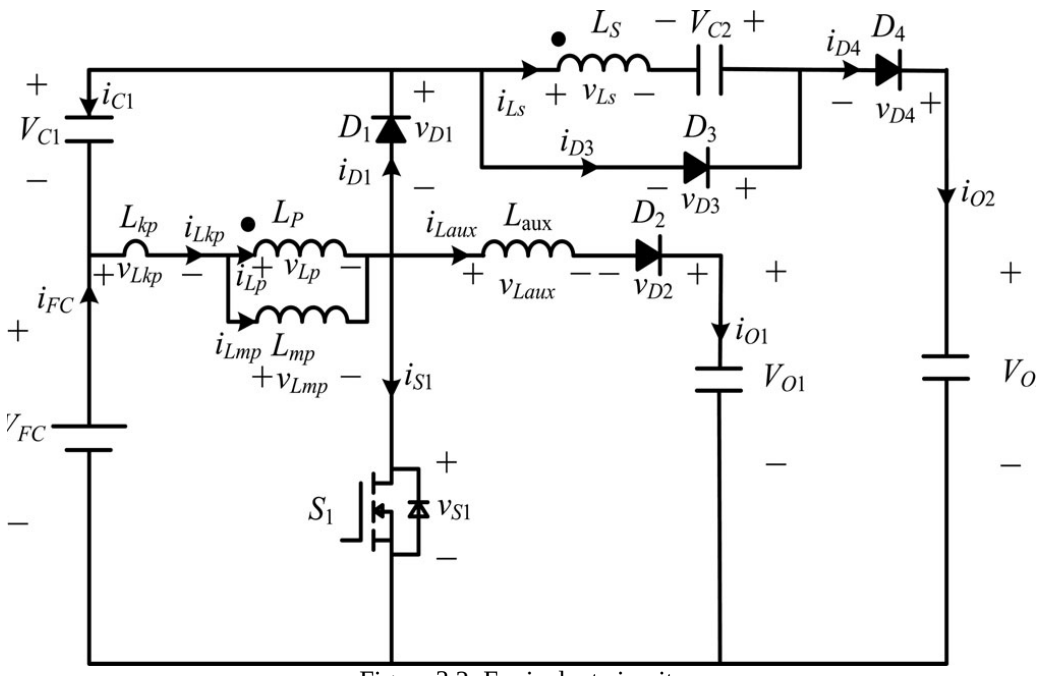

Figure 3.2: Equivalent circuit.

IV. OPERATION MODES

The characteristic waveforms are depicted in Fig. 3, and the topological modes in one switching cycle are illustrated in Fig.3.1

4.1 Mode 1

Mode 1 (t_0–t_1) [Fig. 3.1(a)]: In this mode, the main switch S1 was turned ON for a span, and the diode D_4 turned OFF. Because the polarity of the windings of the coupled inductor Tr is positive, the diode D_3 turns ON. The secondary current i_{L_S} reverses and charges to the middlevoltage capacitor C_2. When the auxiliary inductor L_{aux} releases its stored energy completely, and the diode D_2 turns OFF, this mode ends.

4.2 Mode 2

Mode 2 (t1 –t2) [Fig. 3.1(b)]: At time t = t_1 , the main switch s_1 is persistently turned ON. Because the primary inductor L_p is charged by the input power source, the magnetizing current $i_{L_{mp}}$ increases gradually in an approximately linear way. At the same time, the secondary voltage v_{L_S} charges the middle-voltage capacitor C_2 through the diode D_3 . Although the voltage $v_{L_{mp}}$ is equal to the input voltage v_{FC} both at modes 1 and 2, the ascendant slope of the leakage current of the coupled inductor (di_{Lkp} /dt) at modes 1 and 2 is different due to the path of the auxiliary circuit. Because the auxiliary inductor Laux releases its stored energy completely, and the diode D_2 turns OFF at the end of mode 1, it results in the reduction of di_{Lkp}/dt at mode 2.

4.3 Mode 3

Mode 3 (t_2 –t_3) [Fig. 3.1(c)]: At time t = t_2 , the main switch S1 is turned OFF. When the leakage energy still released from the secondary side of the coupled inductor, the diode D_3 persistently conducts and releases the leakage energy to the middle-voltage capacitor C_2 . When the voltage across the main switch v_{s1} is higher than the voltage across the clamped capacitor V_{c1} , the diode D_1 conducts to transmit the energy of the primary-side leakage inductor L_{kp} into the clamped capacitor C_1 .At the same time, partial energy of the primary-side leakage inductor L_{kp} is transmitted to the auxiliary inductor Laux, and the diode D_2 conducts. Thus, the current i_{Laux} passes through the diode D_2 to supply the power for the output load in the auxiliary circuit. When the secondary side of the coupled inductor releases its leakage energy completely, and the diode D_3 turns OFF, this mode ends.

4.4 Mode 4

Mode 4 (t_3–t_4) [Fig. 3.1(d)]: At time t = t_3 , the main switch S_1 is persistently turned OFF. When the leakage energy has released from the primary side of the coupled inductor, the secondary current i_{LS} is induced in reverse from the energy of the magnetizing inductor Lmp through the ideal transformer, and flows through the diode D_4 to the HVSC. At the same time, partial energy of the primary side leakage inductor L_{kp} is still persistently transmitted to the auxiliary inductor Laux, and the diode D_2 keeps to conduct. Moreover, the current i_{Laux} passes through the diode D_2 to supply the power for the output load in the auxiliary circuiti_{Laux} .

4.5 Mode 5

Mode 5 (t_4 –t_5) [Fig. 3.1(e)]: At time t = t_4, the main switch S_1 is persistently turned OFF, and the clamped diode D_1 turns OFF because the primary leakage current i_{Lkp} equals to the auxiliary inductor current i_{Laux} . In this mode, the input power source, the primary winding of the coupled inductor Tr , and the auxiliary inductor Laux connect in series to supply the power for the output load in the auxiliary circuit through the diode D_2 . At the same time, the input power source, the secondary winding of the coupled inductor Tr , the clamped capacitor C_1 , and the middlevoltage capacitor (C_2) connect in series to release the energy into the HVSC through the diode D_4 .

4.6 Mode 6

Mode 6 (t_5 –t_6) [Fig. 3.1(f)]: At time t=t_5 , thismode begins when the main switch S_1 is triggered. The auxiliary inductor current i_{Laux} needs time to decay to zero, the diode D_2 persistently conducts. In this mode, the input power source, the clamped capacitor C_1 , the secondary winding of the coupled inductor Tr , and the middle-voltage capacitor C_2 still connect in series to release the energy into the HVSC through the diode D_4 . Since the clamped diode D_1 can be selected as a low-voltage Schottky diode, it will be cut off promptly without a reverse-recovery current. Moreover, the rising rate of the primary current i_{Lkp} is limited by the primary-side leakage inductor L_{kp} . Thus, one cannot derive any currents from the paths of the HVSC, the middle-voltage circuit, the auxiliary circuit, and the clamped circuit. As a result, the main switch S_1 is turned ON under the condition of ZCS and this soft-switching property is helpful for alleviating the switching loss. When the secondary current i_{Ls} decays to zero, this mode ends. After that, it begins the next switching cycle and repeats the operation in mode 1.

Remark 1: In general, a dc–dc converter operated at the continuous conduction mode (CCM) can provide a low ripple current for protecting the energy source. In the proposed SIMO converter, it is operated at the CCM due to the design of the auxiliary inductor. The coupled inductor is charged by the input power source when the main switch is turned ON, and the coupled inductor releases its energy to the auxiliary inductor when the main switch is turned OFF until the energy balance of the coupled inductor and the auxiliary inductor is established. As can be seen from Fig. 3, the primary current of the coupled inductor is positive during one switching cycle. This CCM operation is helpful to extend the lifetime of the input energy source.

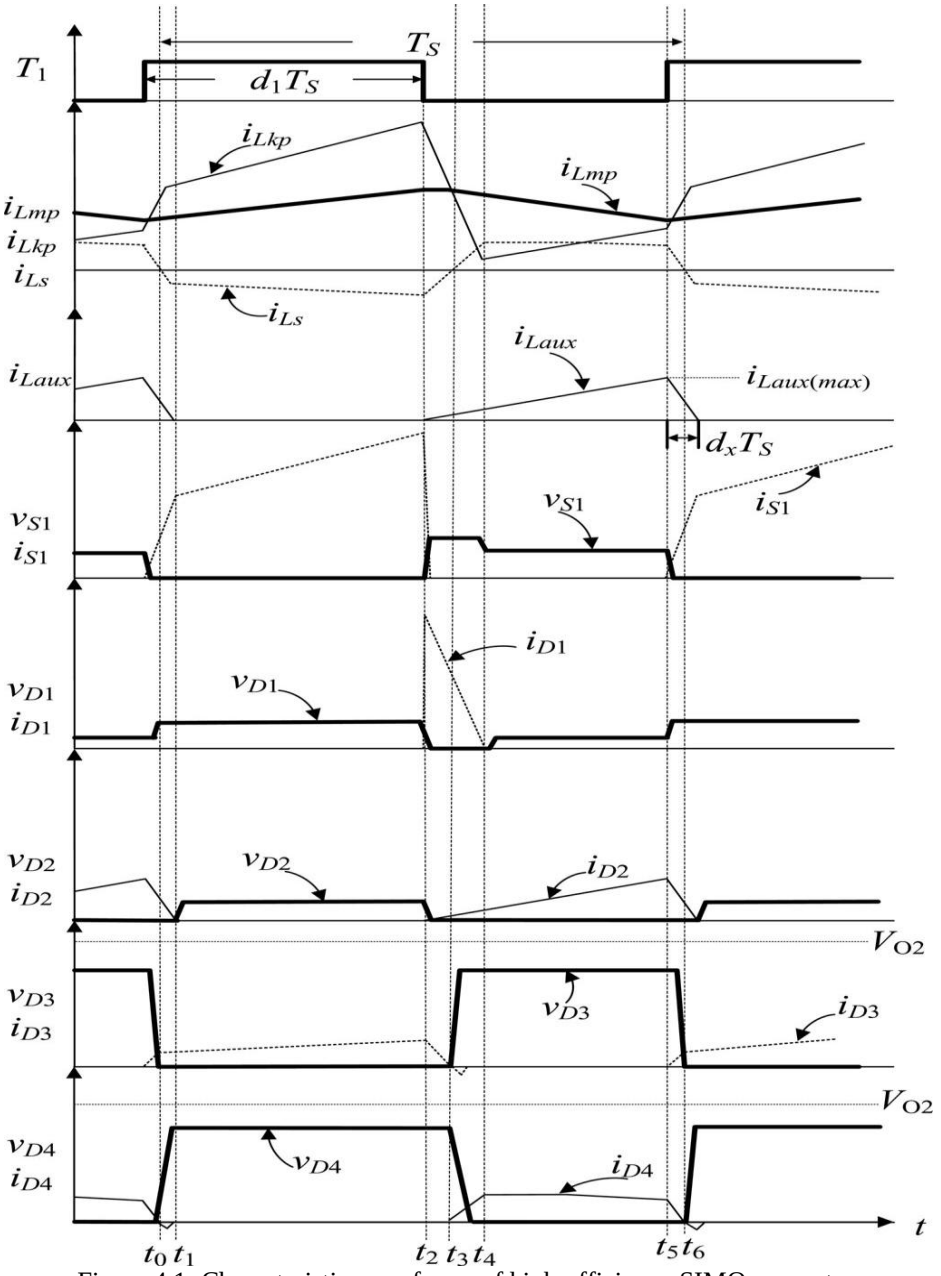

Figure 4.1: Characteristic waveforms of high-efficiency SIMO converter.

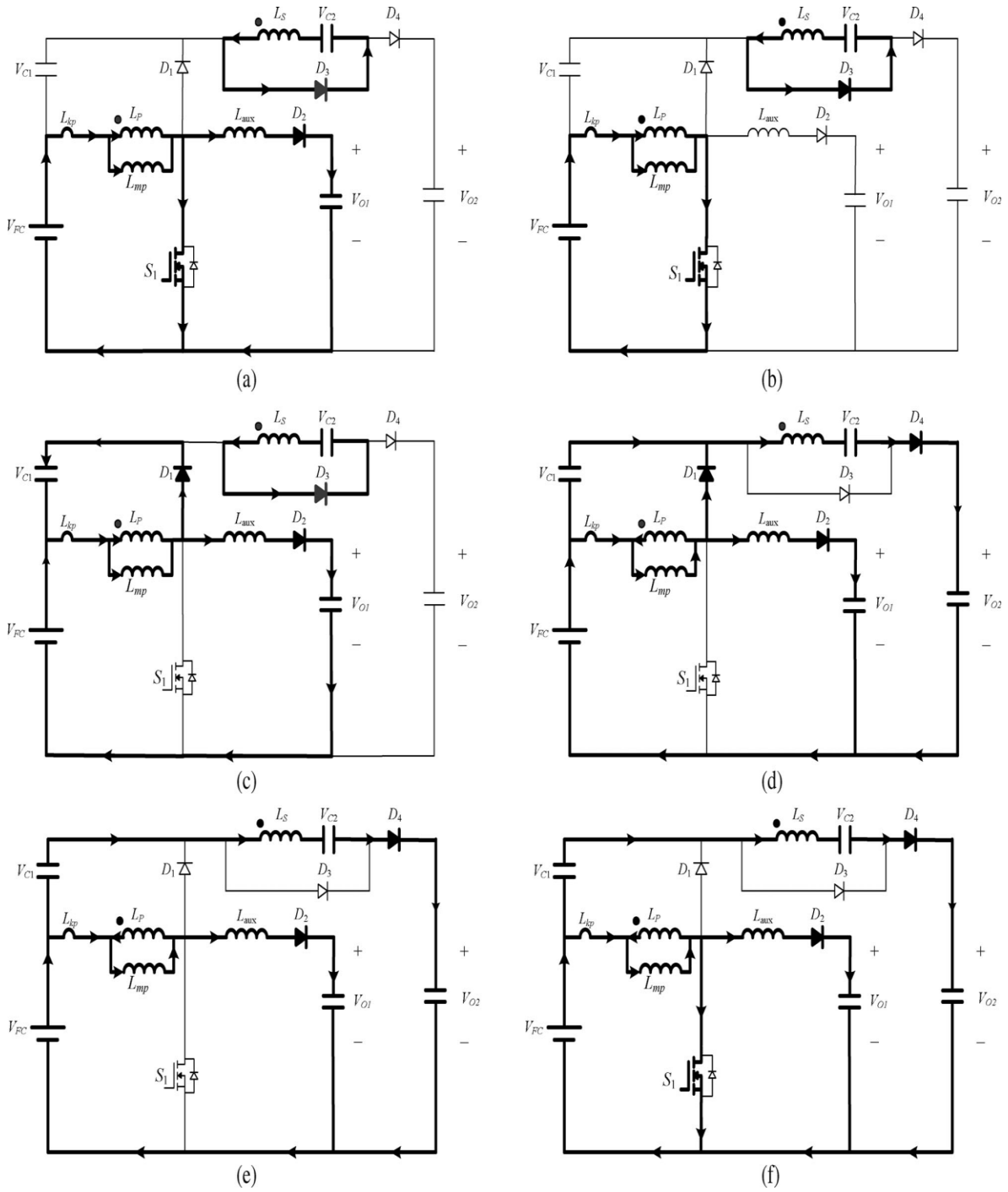

Figure4.2: Topological modes: (a) Mode 1 [$t0$–$t1$]; (b) Mode 2 [$t1$–$t2$]; (c) Mode 3 [$t2$–$t3$]; (d) Mode 4 [$t3$–$t4$]; (e) Mode 5 [$t4$–$t5$]; (f) Mode 6 [$t5$–$t6$].

V. Voltage Gain Derivation

Since the magnetizing inductor voltage v_{Lmp} is equal to the input power source V_{FC} at the mode 2, the voltage v_{Lmp} can be represented as

$$v_{Lmp} = V_{FC} \tag{3}$$

Due to the relation of $v_{LS} = N v_{LP} = V_{C2}$, the voltage V_{C2} can be represented as

$$V_{C2} = N V_{FC}. \tag{4}$$

By using the voltage-second balance , the relation of the average voltage across the magnetizing inductor L_{mp} of the coupled inductor *Tr* to be zero can be represented as

$$V_{FC}\, d_1 T_S + v_{Lmp}\ (1 - T_1)\ T_S = 0. \quad (5)$$

From (5), one can obtain

$$v_{Lmp} = [-d_1 /(1 - d_1)]\, V_{FC}. \quad (6)$$

Since the voltage of the clamped capacitor V_{C1} is equal to the negative voltage of magnetizing inductors voltage VC1 at modes 3 and 4, the voltage V_{C1} can be expressed via (6) as

$$V_{C1} = -\ v_{Lmp} = [d_1\ (1 - d_1)]\ V_{FC} \quad (7)$$

According to Kirchhoff's voltage law, the output voltage V_{02} can be obtained as

$$V_{02} = V_{FC} + V_{C1} + V_{C2} - V_{LS} \quad (8)$$

By using the voltage-second balance , the relation of the average voltage across the secondary winding V_{LS} to be zero can be expressed by (4) and (8) as

$$(N\, V_{FC})\, d_1\ T_S + (V_{FC} + V_{C1} + V_{C2} - V_{02})(1 - d_1)\, T_S = 0 \quad (9)$$

From (4)–(9), the voltage gain G_{VH} of the proposed SIMO converter from the LVSC to the HVSC can be given as

$$G_{VH} = \frac{V_{02}}{V_{FC}} = \frac{N+1}{1-d_1} \quad (10)$$

For calculating the discharge time of the auxiliary inductor at modes 1 and 6, the corresponding time interval can be denoted as $d_x\ T_S = [(t_6 - t_5) + (t_1 - t_0)]$. By using the voltage-second balance , the relation of the average voltage across the auxiliary inductor L_{aux} to be zero can be represented as

$$(V_{FC} - v_{Lmp} - V_{01})(1 - d_1)\, T_S + (-V_{01})\, d_x\ T_S = 0. \quad (11)$$

The voltage gain *G*VL of the proposed SIMO converter from the LVSC to the auxiliary circuit can be obtained by (6) and (11) as

$$G_{VL} = \frac{V_{01}}{V_{FC}} = \frac{1}{1-d_1+d_x} \quad (12)$$

Because the diode current i_{D2} is equal to the current i_{Laux} , the average value of the diode current i_{D2} can be calculated from the third graph in Fig. 3 as

$$i_{D2(avg)} = \left[\frac{1}{2}\ i_{Laux\,(MAX)}(1 - d_1)T_S + \frac{1}{2}\ i_{Laux\,(MAX)} d_x\ T_S\right] \quad (13)$$

where T_S is the converter switching cycle, $i_{Laux\,(MAX)}$ is the maximum current of the auxiliary inductor and can be expressed as

$$i_{Laux\,(MAX)} = \left(\frac{V_{01}}{L_{aux}}\right) d_x\ T_S \quad (14)$$

By substituting (14) into (13), one can obtain

$$i_{D2(avg)} = \frac{V_{01}}{2L_{aux}}\, d_x\ T_S\quad (1 - d_1 + d_x) \quad (15)$$

Because the average current of the diode D_2 is equal to the current i_{01}, it yields

$$i_{D2(avg)} = \frac{V_{01}}{R_{01}} \quad (16)$$

From (15) and (16), the duty cycle d_x can be rewritten as

$$i_{D2(avg)} = \left[\frac{1}{2}\ i_{Laux\,(MAX)}(1 - d_1)T_S + \frac{1}{2}\ i_{Laux\,(MAX)} d_x\ T_S\right] \quad (17)$$

By substituting (17) into (12), the voltage gain G_{VL} of the proposed SIMO converter from the LVSC to the auxiliary circuit can be rearranged as

$$G_{VL} = \frac{V_{01}}{V_{FC}} = \frac{2}{(1-d_1)+\sqrt{(1-d_1)^2+\left[\frac{8L_{aux}}{R_{02}T_S}\right]}} \quad (18)$$

VI. Design Considerations

To verify the effectiveness of the proposed SIMO converter topology, a 12-V power supply *V*FC is taken as the input source to imitate a FC stack, and a 24-V battery module is utilized for the output load in the

auxiliary circuit. Moreover, the maximum battery floating charge voltage is set at 28 V, and the allowable charging power is 100 W (R_{01}= 7.84 Ω). In addition, the desired output voltage V_{02} is set at 200 V in the HVSC, and the maximum output power in the HVSC is 1.1 kW (R_{02}= 36.36 Ω). Define the minimum and maximum output powers in the auxiliary circuit and the HVSC as (P_{1min}, P_{1max}) and (P_{2min}, P_{2max},), respectively. In the case of resistive loads, one can, respectively, obtain the minimum and maximum resistances connected at the auxiliary circuit and the HVSC as

$$(R_{01min} = \frac{G_{vL}{}^2 V_{FC}{}^2}{P_{1max}}, R_{01max} = \frac{G_{vL}{}^2 V_{FC}{}^2}{P_{1min}}) \text{and} (R_{02min} = \frac{G_{VH}{}^2 V_{FC}{}^2}{P_{2max}}, R_{02max} = \frac{G_{VH}{}^2 V_{FC}{}^2}{P_{2min}})$$

according to (10) and (12). Furthermore, this converter is operated with a 100-kHz switching frequency (f_s= 100 kHz), and the coupling coefficient could be simply set at one (k = 1) because the proposed circuit has a good clamped effect.

By substituting N = 1– 7 into (10), the curve of the voltage gain G_{VH} with respect to different duty cycles d_1 is depicted in Fig. 5. Moreover, the curve of the voltage gain G_{vL} with respect to different duty cycles d_1 can be represented as Fig. 6.2 by substituting L_{aux} =1– 7μH, T_S = 10 μs, and R_{01}= = 7.84 Ω into (18). By analyzing Fig. 6.1, the turns ratio of the coupled inductor can be selected as N = 5 when the operational conditions are V_{02} =200V and V_{FC} = 12V (i.e., G_{VH}= 16.67), so that the corresponding duty cycle can be obtained as d_1 = 0.64. This value is reasonable in practical applications. As can be seen from Fig. 3, the relation of d_x < d_1 should be satisfied. According to (5.15), the limit for *L*aux can be calculated as *L*aux < 0.5 $d_1 R_{01} T_S$. By considering V_{FC} = 12V, V_{01} = 28 V, and d_1 =0.64, the value of the auxiliary inductor can be obtained asL_{aux} = 2 μH from Fig.6.2

Figure 6.1 Voltage gain *G*VH with respect to duty cycle *d*1 under different turns ratios.

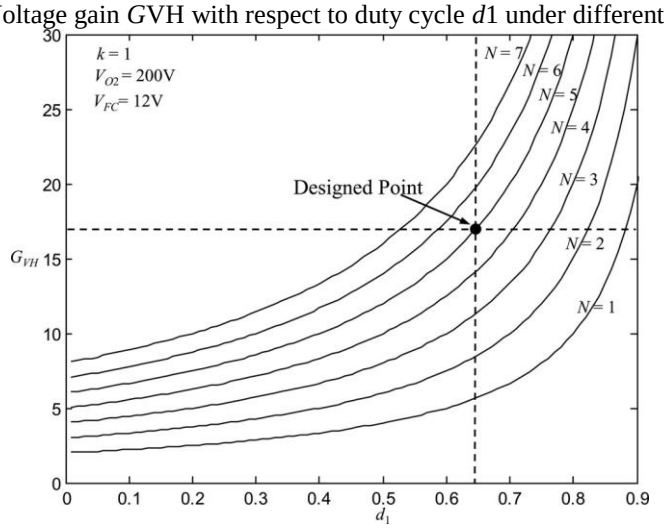

Figure.6.2. Voltage gain GVL with respect to duty cycle *d*1 under different auxiliary inductor values.

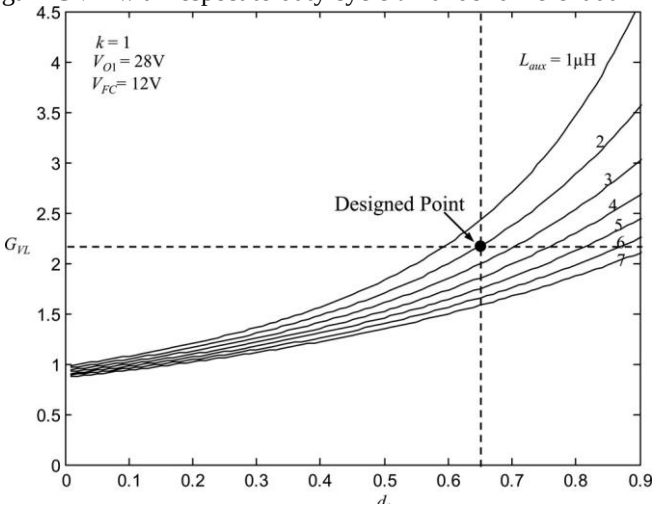

Because the voltage across the main switch S1 at the mode 3 can be represented as $v_{S1} = V_{C1} + V_{FC} = [1/(1 - d_1)]\ V_{FC}$, and the voltage relation between the LVSC and the HVSC according to (10) can be given by $V_{FC} = [(1 - d_1)/(N + 1)]\ V_{02}$, the voltage across the main switch S_1 can be rewritten as

$$v_{S1} = \frac{V_{02}}{N+1} \tag{19}$$

By analyzing (19), the switch voltage V_{S1} is not related to the input power source V_{FC} and the duty cycle d_1 if the values of the output voltage V_{02} and the turns ratio N are fixed. Thus, the switch voltage V_{S1} can be clamped at 33.3 V by substituting N = 5 and V_{02} =200V into (19). As long as the input voltage in the LVSC is not higher than the output voltage in the HVSC, the proposed SIMO converter can be applied well to the input power source with voltage variations. To consider the ring phenomena caused by the circuit stray inductance and the parasitic capacitance of the main switch S_1, the main switch S_1 with a 75-V voltage rating is selected in the proposed SIMO converter.

In this study, the clamped diode D_1 should be a fast conductive device. Because the clamped voltage of the diode D_1 is the same as the one of the main switch S_1, a low-voltage Schottky diode can be adopted to conduct promptly with lower conduction loss and reverse-recovery current. During the mode 2, the diode D_2 turns OFF, and its voltage can be represented by $v_{D2} = V_{01} + [L_{aux}(di_{D2}/d_t)]$. Since the ascendant slope of the diode current (di_{D2}/d_t) is equal to zero at the mode 2, the voltage v_{D2} can be rearranged as $v_{D2} = V_{01}$. According to v_{01}= 28 V, the voltage stress on the diode D_2 is smaller than 100V. Thus, a low-voltage Schottky diode also can be selected to reduce the conduction loss and the reverserecovery current. The voltage across the diodes D_3 and D_4 ,which can be expressed by $v_{D3D4} = v_{02} - (v_{C1} + v_{FC}) = [N/(N+1)]v_{02}$, is 166.67 V by considering N = 5 and v_{02}= 200V. Thus, the diodes (D_3 and D_4) with 200 V voltage ratings can be selected.

When the main switch S_1 is turned ON during modes 1, 2, and 6, the voltage across the magnetizing inductor is $v_{Lmp} = V_{FC}$ = 12V. Moreover, the relation between the current and voltage of the magnetizing inductor can be represented as $v_{Lmp} = L_P(d_i/d_t)$ If the current range *di* is designed as 30 A and $d_t = d_1 T_s$ = 6.4 μs, one can calculate the value of L_P as 2.56 μH. In order to manufacture the couple inductor easily, the number of winding turns in the primary side of the coupled inductor is N_1 = 2, and its measured inductor value is L_P = 3 μH. Because the ratio of the primary and secondary inductors in the coupled inductor is square proportional to the turns ratio (N = 5), the value of L_S can be determined as 75 μH, and the winding turns in the secondary side of the coupled inductor is N_2 = 10 in this study.

In this study, an EE-55 core with the magnetic flux density 390 mT, the maximum magnetic flux 138 μWb, the cross section area 354 mm^2 , and the designed air gap 1.5 mm is adopted as the magnetic core of the coupled inductor. According to the magnetic circuit law , the air resistance can be calculated as 3.4 MΩ. By considering the maximum output power 1.1 Kw with the corresponding conversion efficiency 85%, the maximum input current is about 107.84 A, and the maximum magnetizing current is about 122.84 A. The produced magnetic flux can be obtained as 72.25 μWb by using the primary winding turns (N_1= 2), maximum magnetizing current (122.84 A), and air resistance (3.4MΩ). Thus, the saturation phenomenon of the magnetizing current can be prevented by the designed magnetic core of the coupled inductor.

In the proposed SIMO converter, the electric charge variation Δ*Q*1 of the filter capacitor for the auxiliary circuit can be represented as $\Delta Q_1 = (V_{01}/R_{01})(d_1 - d_x)T_S = C_{01}\Delta V_{01}$. By substituting d_1= 0.64, R_{01} =7.84 Ω, T_s = 10 μs, and L_{aux} = 2 μH into (17), the duty cycle dx can be calculated as 0.11. If one sets the voltage ripple of VO1 to be less than 1%, the value of CO1 should be selected over 67.6 μF by substituting d_1 = 0.64, d_x = 0.11, R_{01}= 7.84 Ω, F_S= 100 kHz, and V_{01} = 28 V into the function of $C_{01} = (d_1 - d_x)/[(R_{01}F_s)(\Delta V_{01}/V_{01})]$. Moreover, the electric charge variation of the filter capacitor Δ*Q*2 for the HVSC can be expressed as Δ*Q*2 =$(V_{02}/R_{02})d_1 T_S = C_{02}c\Delta V_{02}$. and the ripple of the output voltage V_{02} can be rearranged as $\Delta V_{02}/V_{02} = d_1/(R_{02}C_{02}F_s)$. By substituting F_s = 100 kHz, d_1 = 0.64, R_{02}= 36.36 Ω, and V_{02}= 200V into the function of $C_{02} = (d_1)/[(R_{02}F_s)(\Delta V_{02}/V_{02})]$, The value of C_{02} should be chosen over 17.6 μF with the constraint on the output voltage ripple to be less than 1%. According to the previous consideration, the values of C_{01}= 100μF and C_{02}= 20 μF are adopted in the experimental prototype.

Due to a high-switching frequency (F_s = 100 kHz) in the proposed SIMO converter, the factors of lower equivalent series resistance and faster dynamic response should be considered in the design of the clamped capacitor C_1 and the middle-voltage capacitor C_2 for reducing the capacitor voltage ripples. In this study, metalized-polyester film capacitors are adopted for C_1 and C_2 for satisfying the fast charge and discharge property.In order to further minimize the current and voltage ripples imposed to the main switch *S*1 and the diodes D_3 and D_4, the cutoff frequencies of the $L_P - C_1$ and $L_S - C_2$ filters are taken to be at least ten times smaller than the switching frequency. According to the previous consideration, the values of C_1 and C_2 are, respectively, chosen as 85 and 10 μF in theproposed SIMO converter so that the corresponding resonant frequencies are $F_{01} \equiv 1/\left(2\pi\sqrt{L_P C_1}\right) \cong 9.97\text{kHZ}.$ and $F_{02} \equiv 1/\left(2\pi\sqrt{L_S C_2}\right) \cong 5.81\text{kHZ}.$

According to (6.1), the switch voltage v_{S1} can be effectively clamped at a predetermined value if the values of the output voltage V_{02} and the turns ratio N are fixed. As can be seen from Fig. 4.2(a) and (f), the action of the auxiliary circuit is helpful to share the switch current iS1 . For the proposed SIMO converter with larger output powers and more than two outputs, the increase of the input current will raise the current stress on the main switch. Fortunately, one can use the parallel MOSFET to reduce the conduction loss of the main switch.

VII. Simulation Results

Simulation is done on MATLAB/Simulink background

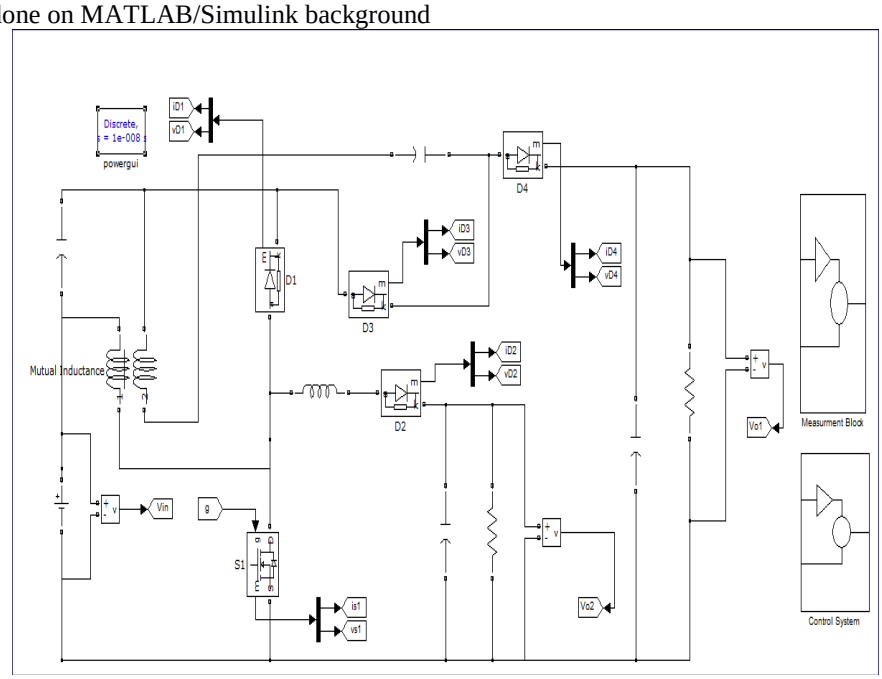

PI Controller

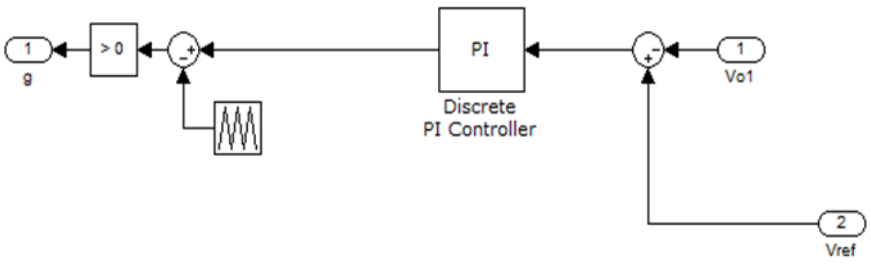

Simulation results of the circuit

7.1 voltage waveforms

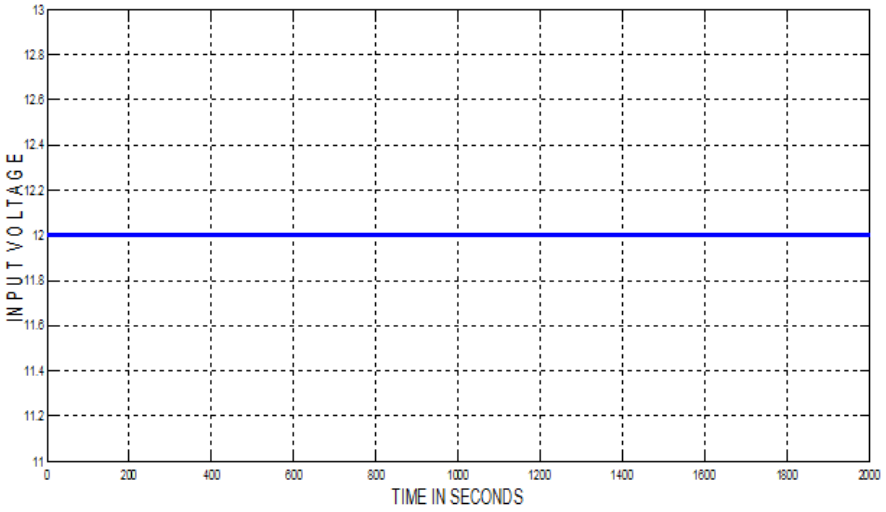

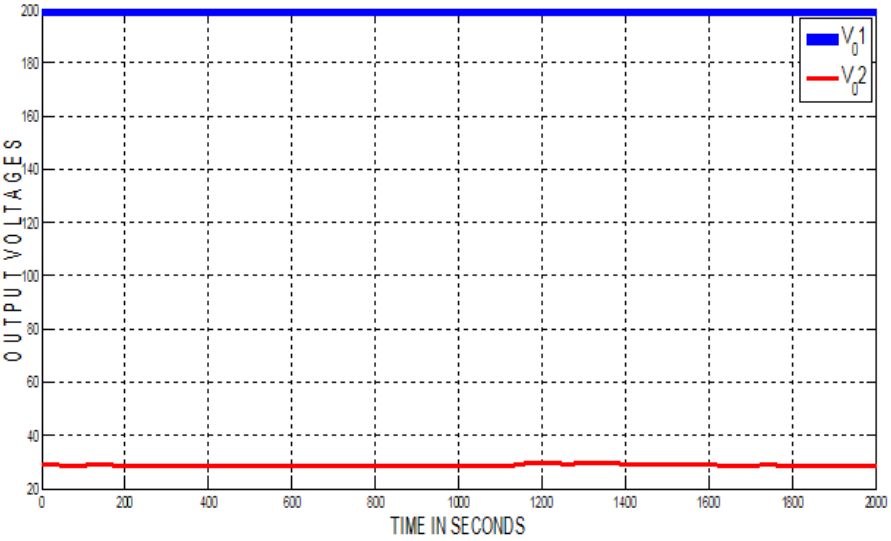

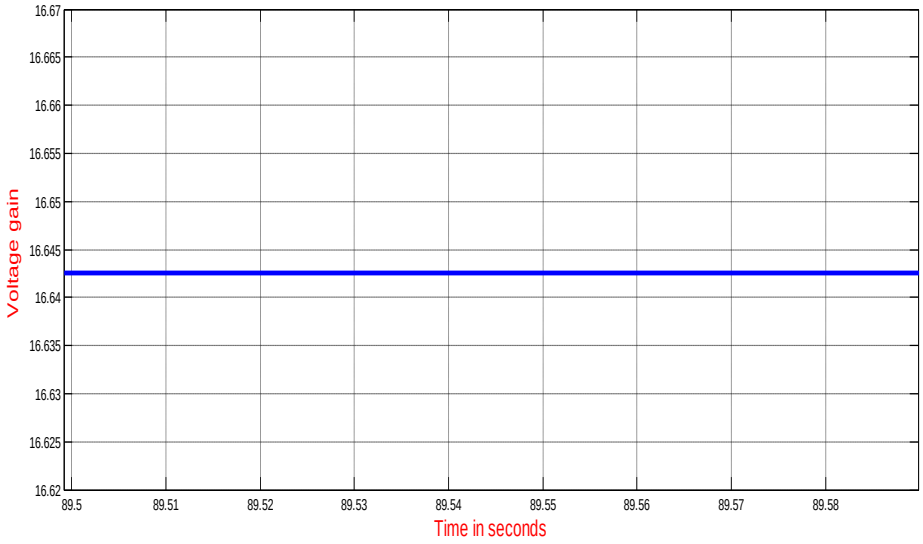

7.2 Voltage & current waveforms across diode

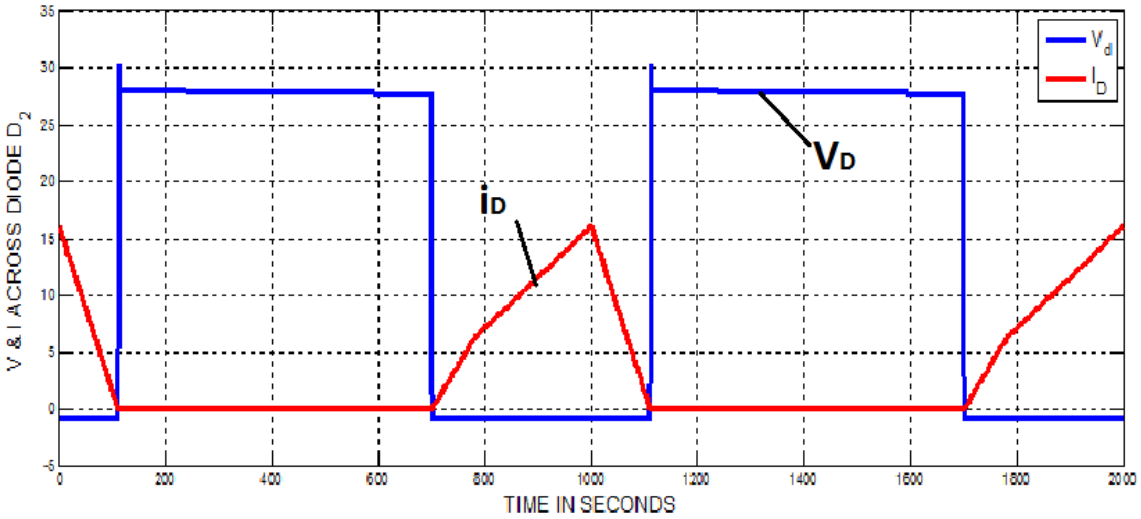

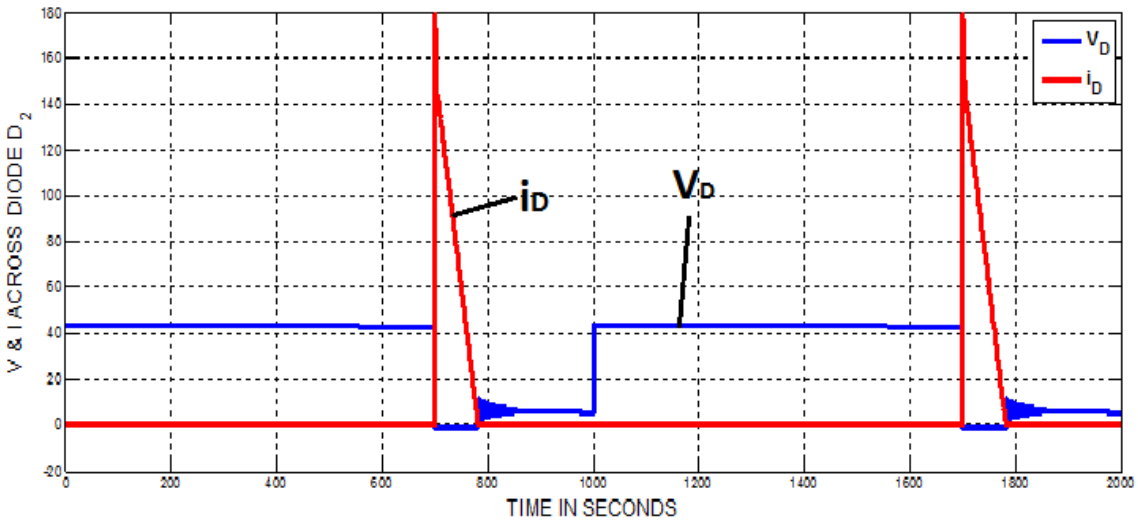

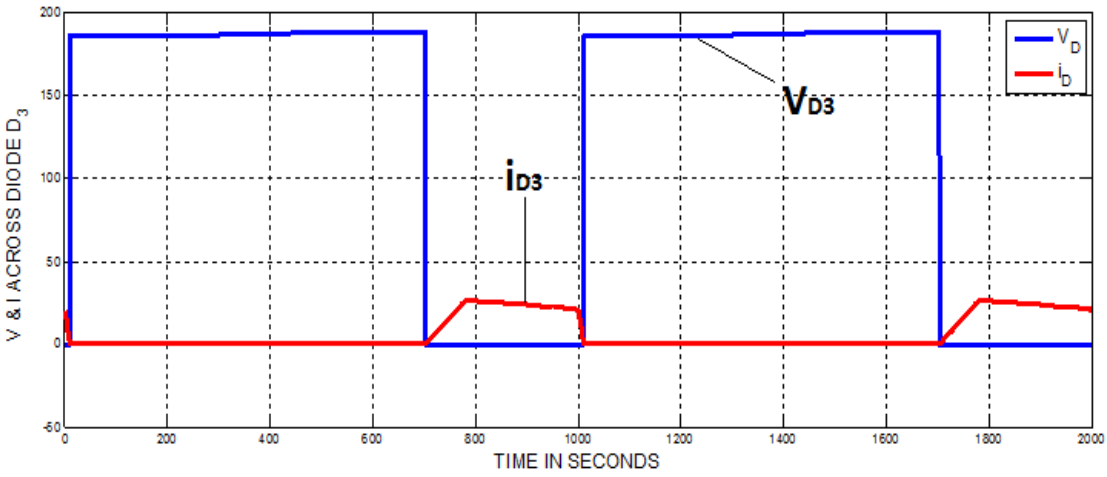

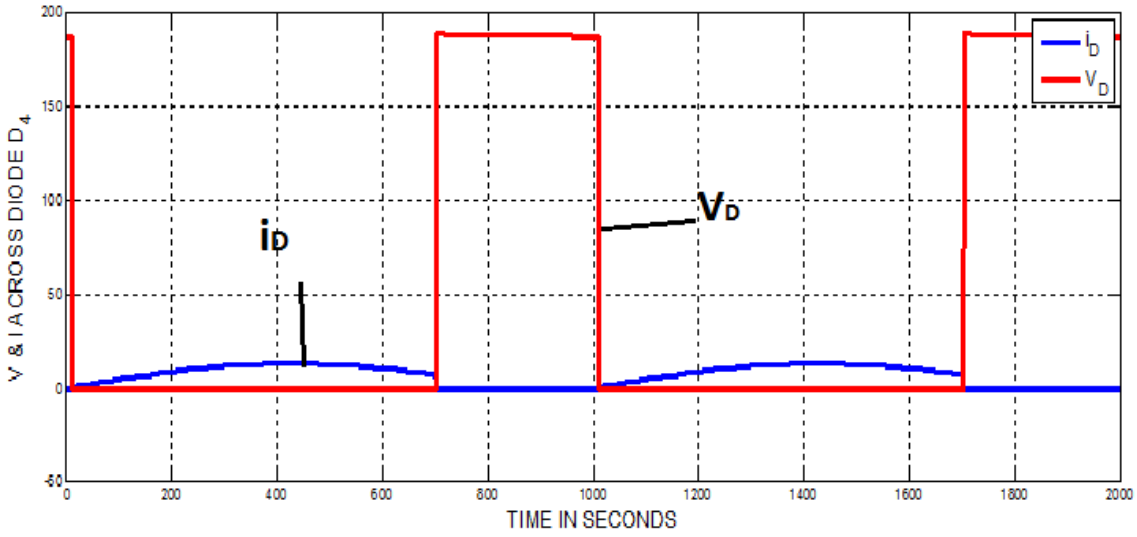

7.3 Voltage & current waveforms across switch

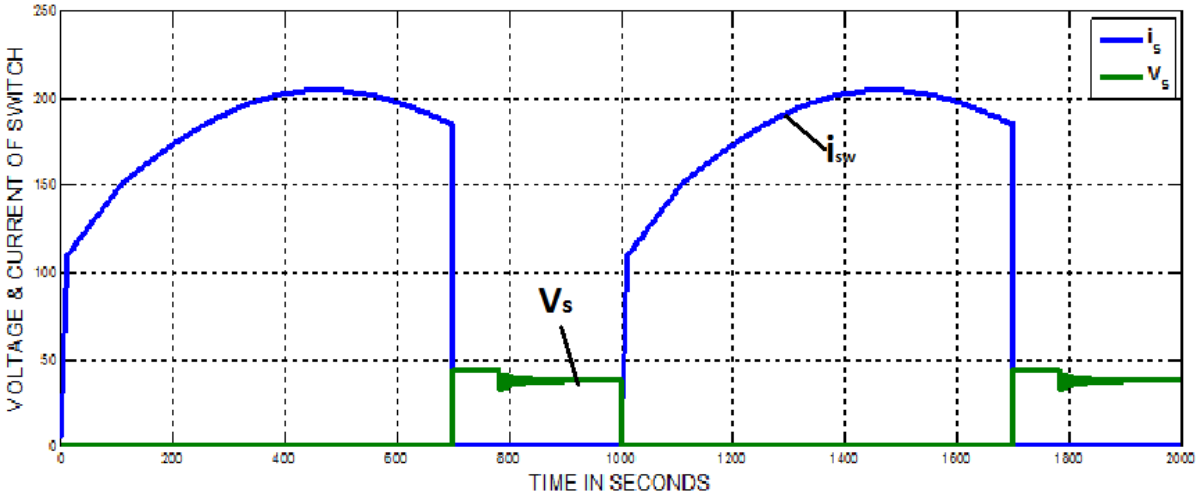

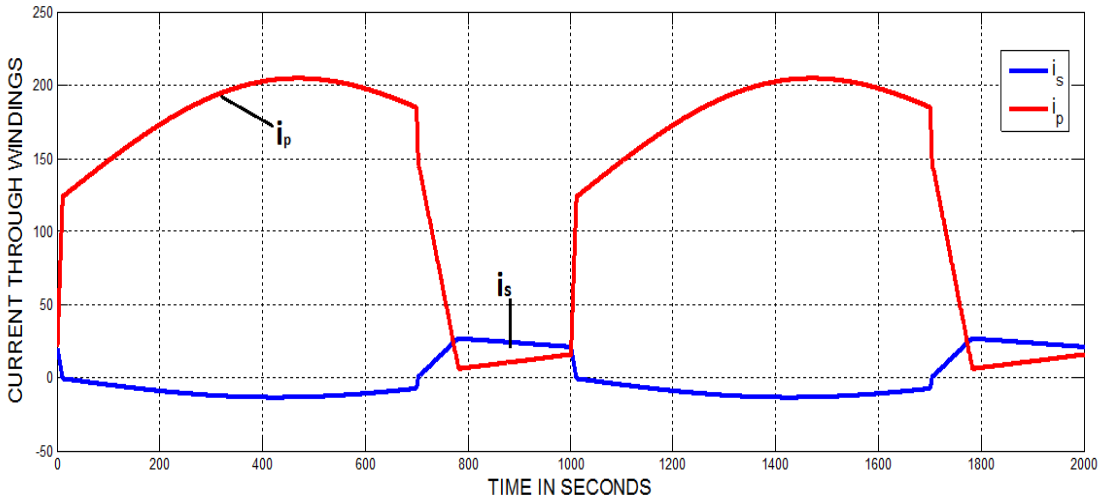

VIII. Conclusion

This study has successfully developed a high-efficiency SIMO dc–dc converter, and this coupled-inductor-based converter was applied well to a single-input power source plus two output terminals composed of an auxiliary battery module and a high-voltage dc bus. The experimental results reveal that the maximum efficiency was measured to exceed 95%, and the average conversion efficiency was measured over 91%. The proposed SIMO converter is suitable for the application required one common ground, which is preferred in most applications.However, it is not appropriate to be used as the active front for dc–ac multilevel inverters. This limitation is worthy to be investigated in the future research.The major scientific contributions of the proposed SIMO converter are recited as follows:

1) this topology adopts only one power switch to achieve the objective of high-efficiency SIMOpower conversion; 2) the voltage gain can be substantially increased by using a coupled inductor; 3) the stray energy can be recycled by a clamped capacitor into the auxiliary battery module or high-voltage dc bus to ensure the property of voltage clamping; 4) an auxiliary inductor is designed for providing the charge power to the auxiliary battery module and assisting the switch turned ON under the condition of ZCS; 5) the switch voltage stress is not related to the input voltage so that it is more suitable for a dc power conversion mechanism with different input voltage levels; and 6) the copper loss in the magnetic core can be greatly reduced as a full copper film with lower turns.

REFERENCE

[1] Rong-Jong Wai, and Kun-Huai Jheng, "High-Efficiency Single-Input Multiple-Output DC–DConverter" EEE Trans.Power Electron., vol. 28, no. 2, pp. 3853–3864, Feb. 2013.

[2] A. Nami, F. Zare, A. Ghosh, and F. Blaabjerg, "Multiple-output DC–DCconverters based on diode-clamped converters configuration: Topology and control strategy," IET Power Electron., vol. 3, no. 2, pp. 197–208, 2010.

[3] M. Singh and A. Chandra, "Application of adaptive network-based fuzzy interference system for sensorless control of PMSG-based wind turbinewith nonlinear-load-compensation capabilities," IEEE Trans. Power Electron.,vol. 26, no. 1, pp. 165–175, Jan. 2011.

[4] C. T. Pan,M. C. Cheng, and C.M. Lai, "A novel integrated dc/ac converter with high voltage gain capability for distributed energy resource systems,"IEEE Trans. Power Electron., vol. 27, no. 5, pp. 2385–2395, May 2012.

[5] S. D. Gamini Jayasinghe, D. Mahinda Vilathgamuwa, and U. K. Madawala, "Diode-clamped three-level inverter-based battery/ supercapacitor direct integration scheme for renewable energy systems," IEEE Trans. Power Electron., vol. 26, no. 6, pp. 3720–3729, Dec.2011.

[6] H.Wu, R. Chen, J. Zhang, Y. Xing, H. Hu, and H. Ge, "A family of threeport half-bridge converters for a stand-alone renewable power system," IEEE Trans. Power Electron., vol. 26, no. 9, pp. 2697–2706, Sep. 2012.